DIRECT MEASUREMENTS OF COSMIC RAYS

Roberta Sparvoli

Università di Roma Tor Vergata and INFN

Lecture 1

INTERNATIONAL SCHOOL OF COSMIC-RAY ASTROPHYSICS MAURICE M. SHAPIRO

24rd Course: "Particles and the Cosmos - Bridging the Infinitesimal and the Infinite" — 29 July - 6 August 2026

Outline of Lecture 1

In this first lecture, we will talk about:

- Spectrum and Composition of Cosmic Rays
- Low-Energy Cosmic Rays: effects of the Sun and the Earth
- Main research lines & platforms for direct detection
- Cosmic Rays measurements: observational strategies
- Main balloon experiments (past and present)
- Main satellite and Space Station experiments (past and present)

The Energy Spectrum of Cosmic Rays

Flux of highly energetic particles, with energies from the MeV range to 10^{20} eV and above.

- Primary component arriving on the top of the atmosphere includes all **stable charged particles and nuclei**.
- The **energy spectrum of CRs** is measured as the **number of particles over area, solid angle, energy bin and time.**
- "All-particle" spectrum

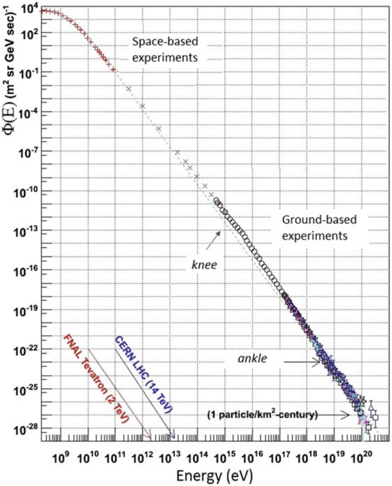

The Energy Spectrum of Cosmic Rays

The energy spectrum **falls steeply as a function of energy**. If we consider isotropic the CR flux, we can integrate the integral flux over the solid angle.

$$\mathscr{F}(>10^9\ \mathrm{eV}) \simeq 1{,}000\ \mathrm{particles/s\ m^2}$$
$$\mathscr{F}(>10^{15}\mathrm{eV}) \simeq 1\mathrm{particle/year\ m^2}$$
$$\mathscr{F}(>10^{20}\mathrm{eV}) \simeq 1\mathrm{particle/century\ km^2}.$$

The energy spectrum of cosmic rays seems almost featureless, but **two transition points are clearly visible**:

• The transition point at $\sim 10^{16}$ eV is called the **knee**. The flux becomes steeper in this region.

• At the energy of 4×10^{18} eV the spectrum becomes flatter again in correspondence of the second transition point, called the **ankle**.

The Energy Spectrum of Cosmic Rays

At energies larger than few GeV **the energy spectrum can be described by a power-law**:

$$\Phi(E) = K\left(\frac{E}{1\text{ GeV}}\right)^{-\alpha} \quad \frac{\text{particles}}{\text{cm}^2\text{ s sr GeV}}$$

The parameter α is the differential spectral index of the cosmic ray flux (or the slope of the CR spectrum) and K a normalization factor.

Different data to determine the parameters K, α are agreement within ~ 30%.

In the energy range from several GeV to 10^{16} eV (the "knee"):

$$\alpha = 2.7 \qquad\qquad E < E_{knee} = 10^{16} eV$$

The Energy Spectrum of Cosmic Rays

Above the "knee" the spectrum becomes steeper, :

$$\alpha = 3.1 \qquad E_{knee} < E < E_{ankle}$$

before hardening again above the "ankle" at $\sim E_{ankle} = 4 \times 10^{18}$ eV :

$$\alpha = 2.7 \qquad E_{ankle} < E < E_{GZK}$$

After $E_{GZK} = 4 \times 10^{19}$ eV the spectra measured by ground experiments appear to fall off. This is pamaretrized by the spectral index:

$$\alpha = 4.2 \qquad E > E_{GZK} = 4 \times 10^{19} eV$$

The so-called **Greisen-Zatsepin-Kuzmin (GZK) effect** foresees that **the proton component of the CR flux from sources at cosmological distances drops sharply above the threshold energy E_{GZK}.**

Composition of Cosmic Rays

We can disentangle the contribution of the different species:

- about 86% are free protons
- about 11% are alpha particles
- 1% are nuclei of heavier elements up to uranium
- 2% are electrons
- a small percentage of positrons and antiprotons

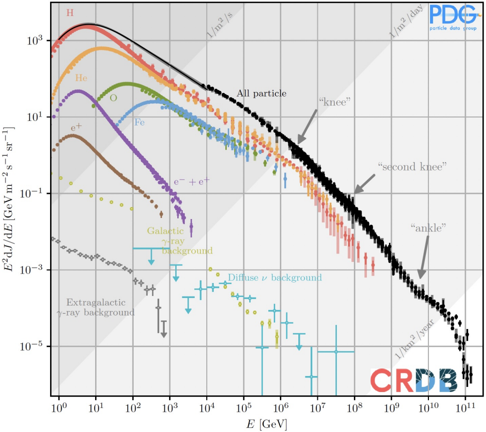

The small flux of electrons does not corresponds to a charge-asymmetry in the CR sources. Electrons suffer larger energy losses that reduce the number of those arriving with high energies on Earth.

Composition of Cosmic Rays

Abundance of the CRs with that of the Solar System: the two samples exhibit a striking similarity:

Odd-even effect: nuclei with Z and A even are most tightly bound than those with odd A and/or odd Z, so more frequently produced in stars. The normalized peaks in C, N, O, Fe are also similar, suggesting that **the cosmic rays are also produced in stars**.

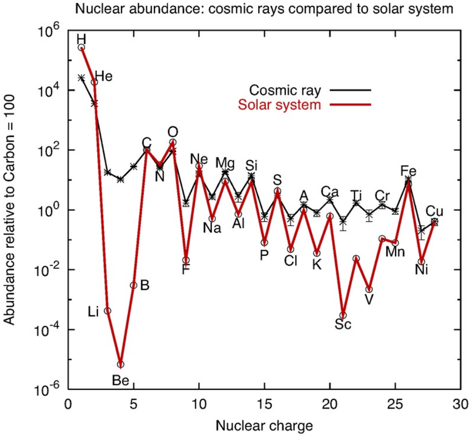

Some remarkable differences between the two exist

Composition of Cosmic Rays

Overabundance of Li, Be, B elements in CRs with respect to the cosmic chemical composition

The ratio (Li+Be+B)/(C+N+O) in CRs exceeds the SS by a factor of $\sim 10^5$. **A similar excess for the elements below the iron ($Z = 26$) and the lead ($Z = 82$) peaks.**

This difference is interpreted as due to the **effect of the propagation in the Galaxy and provide a measure of the material that CRs have encountered since they were accelerated**.
C, N and O are primary cosmic rays, produced and accelerated by astrophysical sources. Li, Be and B are secondary components **produced by spallation** reactions in the interstellar medium.

See talks by P. Mertsch for GCR propagation calculations and more details.

Galactic Cosmic Rays in the Heliosphere

Cosmic rays with energies up to the knee originate in the Milky Way and are therefore called **Galactic cosmic rays (GCRs).** The Sun affects GCRs in two ways:

⋄ **The Sun is the main source of CRs of energy below** $\sim$ **4 GeV**.
Protons, electrons and heavy ions originated mainly by **Solar Flares** and **Coronal Mass Ejections**.
→ *Solar Energy Particle* (*SEP*) events.

⋄ **When GCRs enter our solar system, they must overcome the outward-flowing solar wind**.
This wind is a stream of electrons and protons between 1.5 and 10 keV continuously released from the upper atmosphere of the Sun.

Galactic Cosmic Rays in the Heliosphere

In a **Solar Energy Particle (SEP)** event, fluxes increase by orders of magnitude wrt the flux of Galactic Cosmic rays.

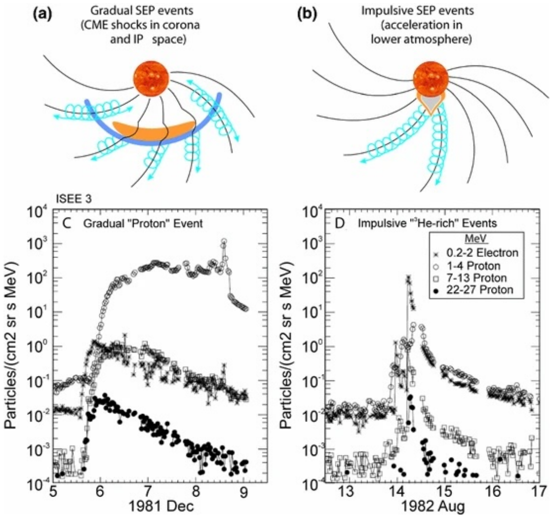

Solar modulation

The expanding magnetized plasma generated by the Sun decelerates and partially excludes the lower energy particles (below $\sim$ 1 GeV/nucleon) from the inner solar system. Consequently the low-energy component of the CR flux undergoes a sizable variation over the solar cycle. This effect is known as **solar modulation.**

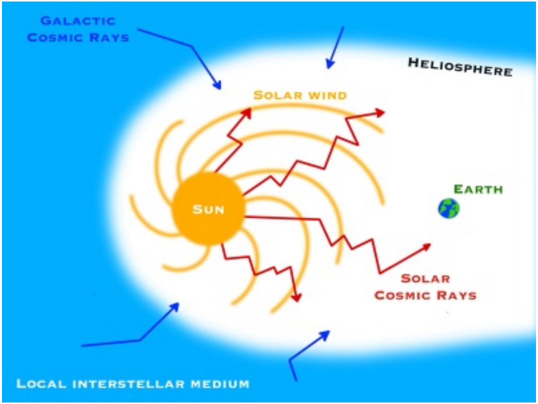

Solar modulation

The intensity of Solar CRs at Earth is measured through ground-based detectors called neutron monitors, measuring neutrons produced by the interactions of CRs with the atmospheric nuclei.

The magnetic activity and the solar modulations are manifested through sunspots, which have a **11 year cycle**.
CR's measurements are anti-correlated with the level of solar activity, i.e., when solar activity is high many sunspots are visible, the CR intensity at Earth is low, and vice versa.

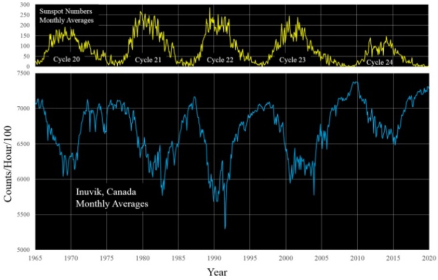

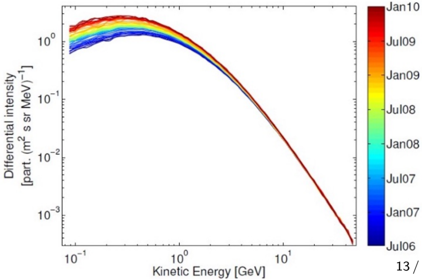

The Earth magnetic field

Originated by electric currents running inside the Earth core.

To a first approximation **it is a dipolar field:**

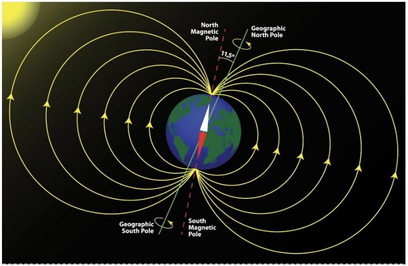

Coordinates: 79° N; 70° W and 79° S; 110° E, reversed with respect to geographic Poles, about 11° inclined with Earth axis and shifted by 320 km.

The field changes slowly over the years, producing a **secular drift of the magnetic Poles.**

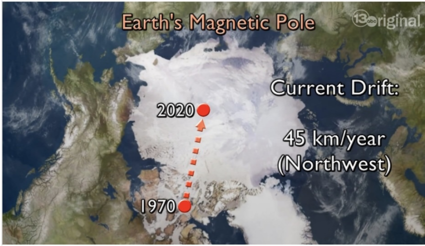

Magnetic field equations: dipole field

The "dipole representation" is accurate to ~ 30% at distances ~ 2-3 R_E.

A better empirical representation is based on a **multipole expansion (International Geomagnetic Reference Field IGRF model)**, with slowly time-dependent coefficients.
To describe the field, also in not-dipole approximation, **McIlwain coordinates (B,L) are used.**

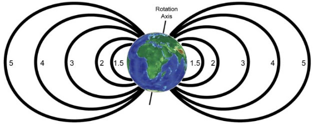

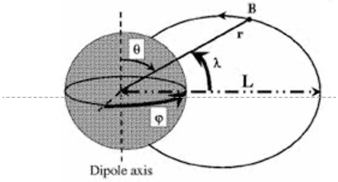

A point P in space is defined by:

L → distance (in R_E) of the field line passing far P, measured on the equatorial plane. A measure of **"equatorial radius".**

B → magnetic field intensity in P. A measure of **"latitude"**.

CRs trajectories in the Earth Magnetic field

Consider a particle of charge Ze with **orbit in the equatorial plane of the dipole-like Earth magnetic field**. Equating the centrifugal and the Lorentz force gives

$$\frac{mv^2}{r} = Ze\,|\mathbf{v} \times \mathbf{B}|$$

The Earth magnetic field is induced by the Earth magnetic moment M:

$$B = \frac{\mu_0}{4\pi}\frac{M}{r^3}$$

At the surface ($r = R_E = 6.38 \times 10^6 m$) the measured value is $B = 0.307 \times 10^4$ T, therefore $M = 7.94 \times 10^{22} Am^2$. It is easy to work out the radius of the orbit from the 2 previous equations:

$$r = \left(\frac{\mu_0}{4\pi}\frac{Ze\,M}{p}\right)^{1/2}$$

where p is the particle momentum.

CRs trajectories in the Earth Magnetic field

Using the numerical values for the Earth's radius:

$$\frac{p}{Ze} = \frac{\mu_0}{4\pi}\frac{M}{R_E^2} \sim 59.6\ GV$$

where GV stands for Gigavolt and it is a measure of the **particle's rigidity**.
This value corresponds to the **minimum rigidity for a particle to be able to reach the Earth**, if its orbit is exactly in the (magnetic) equatorial plane. This value is called **equatorial cut-off rigidity**.

Toward the poles, the influence of the dipole field becomes weaker (as the arriving particle velocity is almost parallel to B), and **the cutoff rigidity becomes smaller.** Thus the integrated CR intensity **increases with the latitude for charged particles (latitude effect).**

CRs trajectories in the Earth Magnetic field

Let us consider a particle with Z and **p** detected at a point **x**; we can **trace back the particle path to its origin**:

a) the trajectory originates from Earth's surface or in atmosphere;

b) the trajectory remains confined in the volume $R_E < r < \infty$;

c) the trajectory reaches infinity.

Trajectories a) and b) are **"forbidden"** because no cosmic rays from far away can reach the Earth along them.
The others are **"allowed"**. Positive particles with rigidity higher than the cut-off are allowed.

The effect of the geomagnetic field is to remove particles from the forbidden trajectories, without deforming their spectrum.

Van Allen Belts: discovery

No attention was given to the "forbidden" orbits, though mathematically known, **until they were truly discovered (Van Allen, Explorer I and II, 1958)**.
The Geiger counters onboard above 2000 km seemed to stop working → saturation!

The existence of two radiation belts around the Earth was discovered;

the internal (Inner Belt) full of protons, the external (Outer Belt) rich of electrons.

Van Allen Belts: origin and death

Origin: high energy CR interactions in atmosphere, producing neutrons and then protons and electrons (**CRAND mechanism**).
Also Solar Wind and influences the ionosphere.

Inner Radiation Belt:
protons with E up to hundres of MeV.
Mean life time: years.
Outer Radiation Belt:
electrons with E of a few MeV.
Mean life time: days.

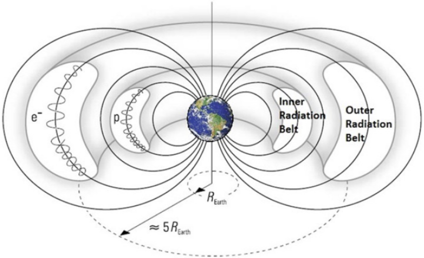

Death: distortions in the magnetic field (also due to solar activity) bring particles to jump to different field lines which go down to denser atmosphere.
Collisions among particles.

Van Allen Belts: particles motion

Combination of 3 periodic motions:

⋄ **Gyration:** a helix around the field line;

⋄ **Bounce:** oscillation around the equatorial plane between almost symmetrical mirror points. Only small oscillations are possible, the mirror point cannot hit the Earth surface.

⋄ **Drift:** longitudinal. It is due to dishomogeneity of the field and variations of the gyroradius. Positive particles drift westward, negative eastward.

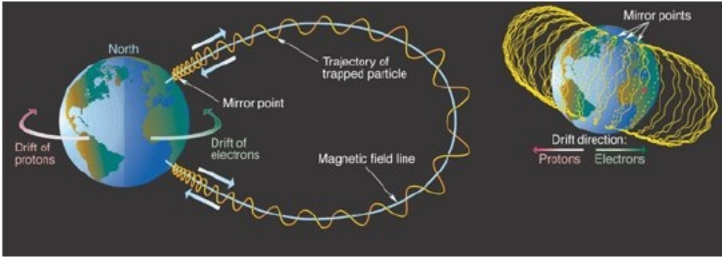

South Atlantic Anomaly SAA

Above South America, about 200 - 300 kilometers off the coast of Brazil, and extending over much of South America, the nearby portion of the Van Allen Belt forms what is called the **South Atlantic Anomaly**.

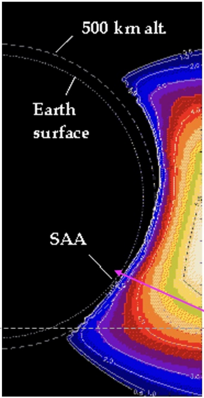

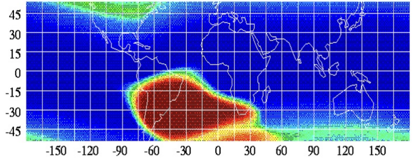

This is an area of **enhanced radiation** caused by the offset and tilt of the geomagnetic axis with respect to the Earth's rotation axis, which brings part of the radiation belt to **lower altitudes**.

The inner edge of the proton belt dips below the line drawn at 500 km altitude.

Direct measurement of Cosmic Rays

Going back to the spectrum of Cosmic Rays, the detection is divided in:

• E < 100 TeV: **direct detection**, by space- and balloon-borne experiments above Earth's atmosphere, in which the primary particles are mostly absorbed.
This detection mainly concerns Galactic Cosmic Rays!

CR fluxes are **influenced by the galactic interstellar medium and magnetic field.** At energies above 30 GeV, **the radiation appears to be isotropic, since the galactic magnetic fields would destroy any initial anisotropy.** → No astronomy with GCRs!

• E > 100 TeV: **indirect detection** by ground-based experiments, which measure air showers of secondary particles produced by the primary cosmic-ray particles interacting in Earth's atmosphere.
This detection mainly concerns Cosmic Rays in transition from the Galaxy out! **Not necessarily isotropic → Sources?**

Main research lines for direct detection

- CR flux reconstruction **up to the highest energy band** (looking for sources and acceleration mechanisms, . . .)
- CR **compositions studies** (looking for source material, dust/gas distribution, nucleosynthesis, selection effects, . . .)
- CR flux **modulation in the low energy band** (looking for effects from heliosphere/magnetosphere, . . .)
- **Antimatter component** in CRs (looking for dark-matter and anti-matter limits, nearby sources, . . .)

It is not possible to study all with the same experiment!

According to the physics line, different detections techniques are adopted

Existing platforms for GCRs detection

- **Balloon experiments**: very popular in the 80's, but later on they were substituted by satellite. They returned popular especially with the NASA Long and Ultra-long Duration Balloon Program.
- **Satellite experiments**: started from 2000. No residual atmosphere but challenging and expensive. Several constraints imposed on experiments.
- **Space station experiments**: similar problematics of satellite, less opportunities to launch.

Why spacecrafts orbits matter

The choice of the spacecraft orbit is very important, since it determines:

- which regions of near-Earth/Solar System space are sampled;
- the particle populations accessible to the detector;
- the geomagnetic cutoff conditions;
- the exposure time and sky coverage;
- the radiation environment experienced by the spacecraft.

For charged-particle measurements, the orbit is not only a technical constraint:

Key idea

The orbit defines the observational window of the experiment.

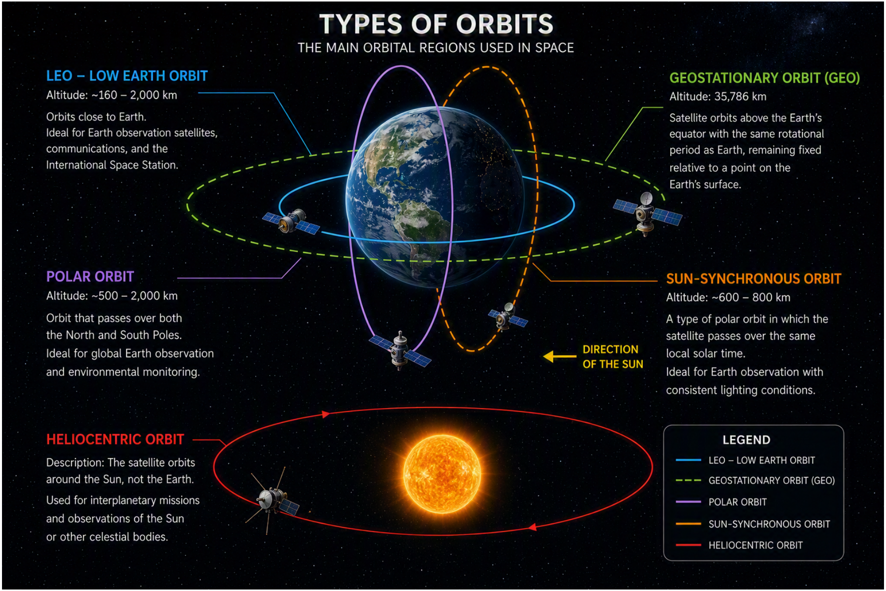
TYPES OF ORBITS
THE MAIN ORBITAL REGIONS USED IN SPACE
LEO – LOW EARTH ORBIT
Altitude: ~160 – 2,000 km
Orbits close to Earth.
Ideal for Earth observation satellites, communications, and the International Space Station.
GEOSTATIONARY ORBIT (GEO)
Altitude: 35,786 km
Satellite orbits above the Earth's equator with the same rotational period as Earth, remaining fixed relative to a point on the Earth's surface.
POLAR ORBIT
Altitude: ~500 – 2,000 km
Orbit that passes over both the North and South Poles.
Ideal for global Earth observation and environmental monitoring.
SUN-SYNCHRONOUS ORBIT
Altitude: ~600 – 800 km
A type of polar orbit in which the satellite passes over the same local solar time.
Ideal for Earth observation with consistent lighting conditions.
DIRECTION OF THE SUN
HELIOCENTRIC ORBIT
Description: The satellite orbits around the Sun, not the Earth.
Used for interplanetary missions and observations of the Sun or other celestial bodies.
LEGEND
LEO – LOW EARTH ORBIT
GEOSTATIONARY ORBIT (GEO)
POLAR ORBIT
SUN-SYNCHRONOUS ORBIT
HELIOCENTRIC ORBIT

What do we need to measure?

To reconstruct a GCR particle fluex, we need to determine:

- Particle identification (charge, sign of the charge, mass);
- Energy spectra;
- Arrival direction and anisotropies;
- Temporal variations.

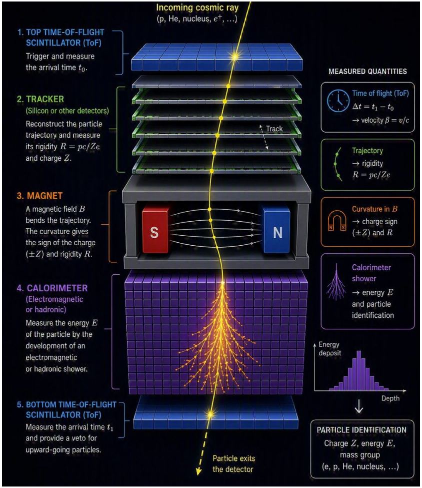

CR measurements: a toy telescope

In order to determine all particle characteristics, a detector must comply with several requirements. Let's take a simple toy telescope to start discussing the main needed parameters.

Layout of a simple telescope for the measurement of CRs. The two counter's *layers* are assumed to be segmented both in the x and y axis. A CR arriving within the *solid angle* $\Delta\Omega$ will produce one hit on each *layer*

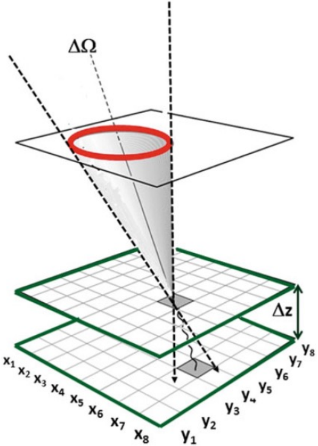

The "hit" recording and Trigger Logic

In the toy telescope a charged particle crossing a sensible layer induces a signal at the position labeled (x_7, y_4). Additional information are the z-position z_1 of the layer, the crossing time (t_1) and the amplitude I_1 of the signal.
The complete set of information **(a hit)** can be represented as $(x_7, y_4; z_1, t_1, I_1)$.

A major requirement of any experiment is the **trigger logic**. This is a **mandatory task**, because the probability of a **fake signal on a single counter is high**.

In our simple example, a trigger is given by a **coincidence between planes**. This corresponds to have a signal both on the z_1 and z_2 layers within a given time interval T. **The hits are permanently stored in the computer for further analysis if** $|t_1 - t_2| \leq T$. A **condition on amplitudes** I_1, I_2 can also be added.
In any experiment, the Trigger Logic defines the requirements necessary for a series of hit signals to be accepted as real event.

Charge identification: dE/dx measurement

The signal in the counter is provided by the excitation/ionization energy loss of through-going charged particles.
The excitation/ionization energy loss is **proportional to the square of the electric charge Z of the particle**. With **proportional counters** the amplitude I_{hit} of the signal depends thus on Z^2.

This method to measure the electric charge of the incoming particle through the Bethe-Bloch formula is referred as **dE/dx measurement**.

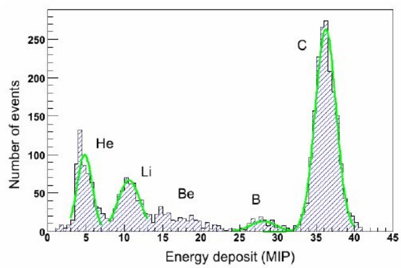

Some experiments have **redundant detectors for the measurement of the electric charge**. This redundancy makes the nuclei selection very clean.

Time-of-Flight (ToF) systems

Basic Principle

Relativistic particles travel in vacuum :

$$1\ \mathrm{m} \simeq 3.3\ \mathrm{ns}$$

For detector spacings of $\Delta z \sim 1-2$ m, a timing resolution of $\sigma_t \lesssim 1$ ns is required.

Main Functions

- Measure the particle flight time
- Determine the particle direction
- Reject upward-going (albedo) particles
- Generate the event trigger
- Estimate the particle charge ($dE/dx \propto Z^2$)

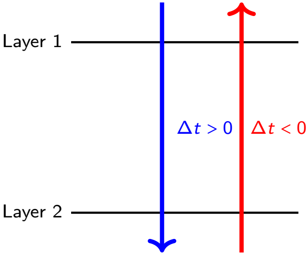

Typical ToF detector:
Plastic scintillator counters

Momentum measurement: magnetic spectrometers

Often a **uniform magnetic field in the region between the counters performing a ToF is present**. The field is generated by a permanent or superconductive solenoid.

The magnetic field allows the measurement of the **particle momentum** (if $|Ze|$ is known), as charged particles are deflected **according to their rigidity** (rigidity: momentum/$|Ze|$), and the **sign of the charge**.

To measure the curved particle trajectory, **additional detectors with good spatial resolution are needed inside the magnetic field region** (tracking system).

The combination of the magnetic field and tracking detectors forms a **magnetic spectrometer**. It can measure the particle rigidity up to a maximum value that depends on the magnetic field and on the precision of the measurement of the curvature. The **maximum detectable rigidity MDR** is reached when the curvatures appear to be straight lines.

Momentum measurement: magnetic spectrometers

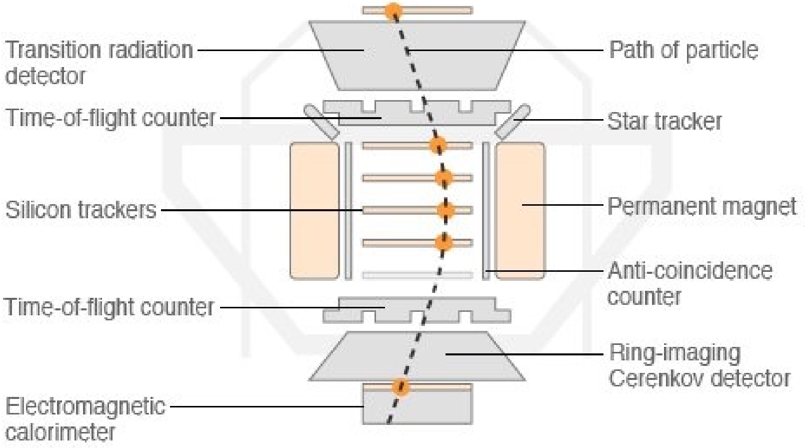

Source: CERN

Velocity measurement: Cherenkov detectors

A precious information about the particle velocity can come from **Cherenkov detectors**.

Cherenkov radiation occurs when **a particle in a medium moves faster than light in the same medium**. **The coherent wavefront has a conical shape and is emitted at an angle**:

$$cos\,\theta = 1/\beta n$$

with respect to the trajectory of the particle.

The dependence of the cone emission angle on the particle velocity is used to construct Cherenkov detectors.

Cherenkov detectors provide precise velocity measurements and, combined with tracking, ToF, and calorimetric information, enable particle identification and mass determination.

Ring-imaging Cherenkov detector

The **Ring-imaging Cherenkov detector (RICH)** estimates the particle velocity $\beta = v/c$ with a high accuracy. The β derives from **pattern recognition of photons distributed over geometrical shapes** as circles, ellipses, arcs produced by the Cherenkov effect. Charge measurement derives from the **total amount of collected photons**. Higher is the charge, higher is the number of photons.

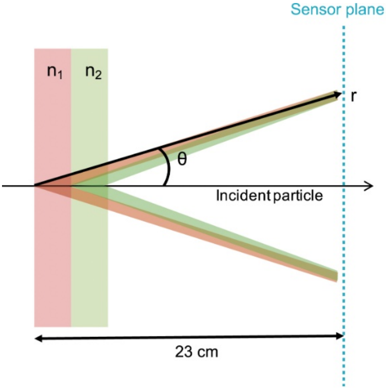

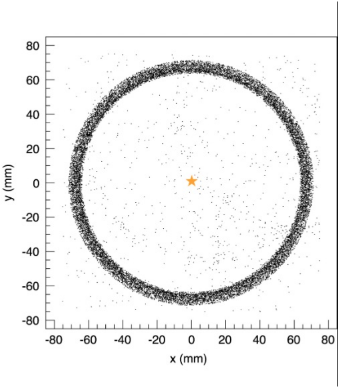

Transition Radiation Detectors TRDs

At high energy, **Transition Radiation Detectors (TRDs)** can be used to measure the Γ Lorentz factor of the incident particle and thus the energy.

Radiation (in the **X-ray band**, called **transition radiation**) is produced when a particle with high Γ crosses several interfaces characterized by a **change of the refraction index**. Particles with large Γ induce X-rays. For a given energy, **this allows a discrimination between light and heavy particle, as** $\Gamma = E/mc^2$.

A TRD contains many layers of transparent materials with **different indices of refraction** n in order to increase the photon emission probability of a single layer.

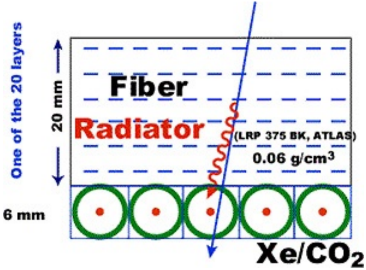

Energy measurement: calorimeters

Basic idea

A calorimeter is a detector designed to measure the energy of a particle by absorbing it and converting its energy into a measurable signal.

- The incoming particle interacts with the detector material and produces a cascade of secondary particles.
- The shower deposits energy through ionization, excitation, and radiation processes.
- The total collected signal is proportional to the incident particle energy:

$$S \propto E_{\mathrm{particle}}$$

Main observables

- Total energy
- Longitudinal and transverse shower profile
- Particle identification from shower topology

Energy measurement: calorimeters

Electromagnetic calorimeters

- Optimized for electrons, positrons, and photons
- Shower mainly driven by:

$$e^{\pm} \to e^{\pm} + \gamma$$

$$\gamma \to e^{+} + e^{-}$$

- Compact and relatively well contained

Hadronic calorimeters

- Used for protons and nuclei
- Showers are more irregular and extended
- Energy reconstruction is complex

Why are they important?

- Extend measurements to high energies
- Improve electron/proton separation
- Provide independent energy measurement
- Complement tracking, TOF and dE/dx systems

Key limitation

Must be sufficiently thick to contain the shower; in space missions this is constrained by mass, volume, and power

How Do We Measure the Mass of a Charged Particle?

The challenge

The mass of a particle is not measured directly. Instead, it is reconstructed from independently measured quantities such as energy, momentum, velocity, or rigidity.

For a non-relativistic particle:

$$E_k = \frac{1}{2} m v^2$$

If both kinetic energy and velocity are measured, the mass can be obtained as

$$m = \frac{2E_k}{v^2}$$

Combining the two observables provides particle identification.

Examples

Isotopes can be distinguished through their reconstructed masses.

Anticoincidence System

Purpose

Help particle containment and reject charged background from the sides:

$$\text{Trigger} = \text{Main detector} \wedge \mathit{NOT}(\mathit{Veto})$$

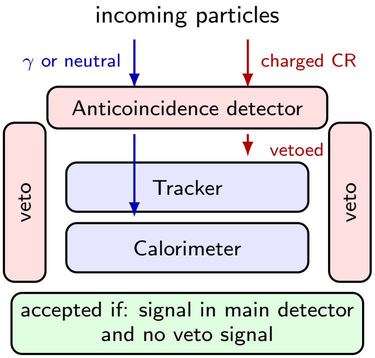

- **Active shield**: usually plastic scintillator panels surrounding the tracker and/or calorimeter.
- **Charged particles**: produce a fast signal in the veto layer and are rejected.
- **Neutral particles**: can enter the main detector without firing the veto.

Major Direct Cosmic-Ray Experiments Since 2000

Mission	Period	Platform
ATIC	2000–2008	Balloon
BESS / BESS-Polar	2004–2007	Balloon
CREAM	2005–2010	Balloon
TRACER	2003–2006	Balloon
SuperTIGER	2012–2019	Balloon
PAMELA	2006–2016	Satellite
Fermi-LAT	2008–present	Satellite
AMS-02	2011–present	ISS
NUCLEON	2014–present	Satellite
CALET	2015–present	ISS
DAMPE	2015–present	Satellite
CSES-01	2018–present	Satellite
ISS-CREAM	2017–2019	ISS
CSES-02	2025–present	Satellite

ATIC and TRACER Balloon Experiments

ATIC (2000–2008)

- Silicon charge detector
- 20 X_0 BGO calorimeter
- Measured CR composition:

$$Z = 1 \rightarrow 26$$

- Since December 2000, 3 successful flights from McMurdo

TRACER (2003–2006)

- 2 layers of Scintillator counters
- Transition Radiation Detector (TRD)
- Measured spectra from:

$$Z = 5 \rightarrow 26$$

- A flight in Antarctica in 2003, and a second flight in 2006.

Key Idea

ATIC pioneered large balloon calorimeters for composition studies, while TRACER demonstrated the use of a large-area TRD for high-energy nuclei measurements.

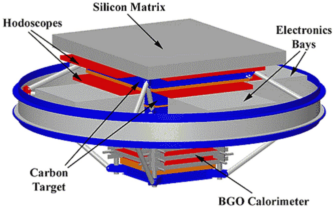
Silicon Matrix
Hodoscopes
Electronics Bays
Carbon Target
BGO Calorimeter

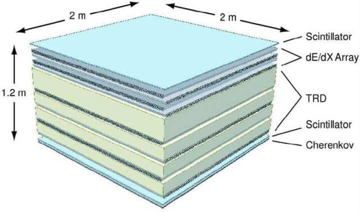
2 m
2 m
1.2 m
Scintillator
dE/dX Array
TRD
Scintillator
Cherenkov

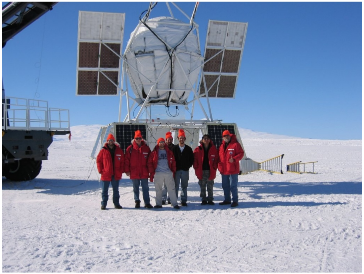

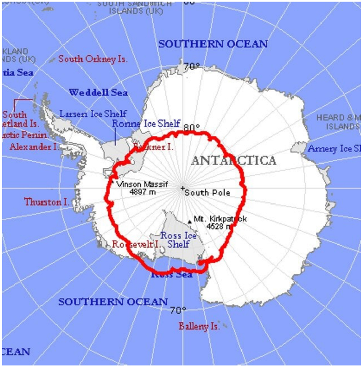
SOUTHERN OCEAN
South Orkney Is.
70°
Weddell Sea
Larsen Ice Shelf
Ronne Ice Shelf
80°
Alexander I.
Vinson Massif
4897 m
South Pole
Thurston I.
Ross Ice Shelf
SOUTHERN OCEAN
70°
Balleny Is.

CREAM Balloon Experiment (2004–2010)

Detector Concept

The **Cosmic Ray Energetics and Mass (CREAM)** experiment combined two independent techniques for measuring the energy of CRs:

- a **Transition Radiation Detector (TRD)**, sensitive to the particle Lorentz factor γ
- a **tungsten/scintillating-fiber calorimeter** (20 radiation lengths, $\sim 0.5\,\lambda_I$), capable of measuring the deposited shower energy.

This unique configuration allowed an **in-flight cross-calibration** of the two methods for nuclei with $Z \geq 4$.

Scientific Achievements

- Direct measurements of cosmic-ray nuclei from H to Fe.
- Extension of elemental spectra up to

$$E \sim 10^{14}\ \mathrm{eV}.$$

Legacy

CREAM completed six long-duration Antarctic balloon flights between 2004 and 2010, accumulating **160 days of exposure**. Its success led directly to the development of the **ISS-CREAM** mission installed on the International Space Station.

a CREAM ballooncraft with the launch vehicle while a 10^6 m^3 balloon is being inflated at the launch site, Williams field near McMurdo, Antarctica; **b** the balloon trajectory of a 37 day flight of CREAM, which was launched on December 1, 2009 and terminated on January 8, 2010 during about three rounds of the South Pole.

SUPER-TIGER: Studying the Origin of Cosmic Rays

Scientific Motivation

SUPER-TIGER (**Super Trans-Iron Galactic Element Recorder**) was designed to measure the composition of **ultra-heavy Galactic cosmic rays**

- Precise measurements of nuclei in the range

$$30 \leq Z \leq 42$$

- Exploratory abundance measurements extending to

$$Z \sim 60.$$

Flights

- Antarctic flight: Dec. 2012 – Jan. 2013. Record duration: 55 days
- Second flight: Dec. 2019 – Jan. 2020. Duration: 32 days

SUPER-TIGER: Instrument and Balloon Flights

Detector Concept

- Plastic scintillator counters
- Acrylic Cherenkov detector
- Aerogel Cherenkov detector
- Scintillating-fiber hodoscope

The combination of charge and velocity measurements provides excellent identification of heavy nuclei.

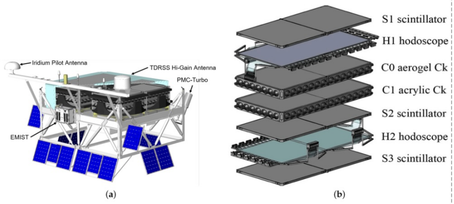

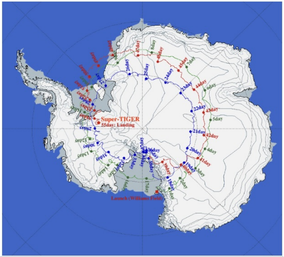

BESS Balloon Experiment (2004 - 2007)

BESS hosts a **superconducting spectrometer**, where a uniform B of about 10^4 G acts for 1 m on the particles. The sagitta is measured by drift chambers. The ToF system provides the measurement of the particle direction, velocity $\beta = v/c$ and Ze.

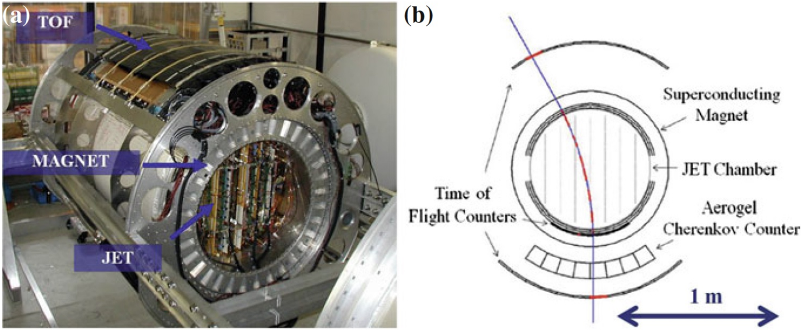

a A picture of the original BESS apparatus. **b** A cross-sectional view of the BESS-Polar instrument showing also a particle trajectory.

BESS Balloon Experiment (2004 - 2007)

BESS has had nine successful flight campaigns since 1993, and additional two over the Antarctica, called BESS-polar.

BESS-Polar I & II flights were carried out over Antarctica.

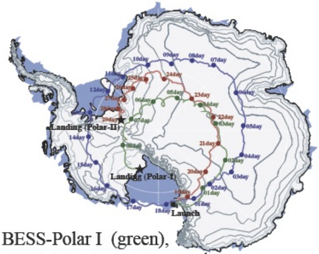

BESS-Polar I (green),
BESS-Polar II (1st :blue, 2nd :red)

	BESS-Polar I	BESS-Polar II
Launch date	Dec. 13th ,2004	Dec. 23rd , 2007
Observation time	8.5 days	24.5 days
Cosmic-ray observed	9×10^8 events	4.7×10^9 events
Flight altitude	37~39km (5~4g/cm^2)	~36km (6~5g/cm^2)

Satellite and Space Station experiments

Starting from the 90's, when the technology was ready, balloon experiments started to be substituted by experiments carried out on **satellites** or on orbiting **Space Stations**.

With respect to balloons, satellite experiments have advantages and disadvantages. Among them we can mention:

- Adv. : much longer data-taking → years instead of days/weeks;
- Adv. : complete absence of residual atmosphere → no necessity to correct the fluxes for the interaction in the upper layers of the atmosphere;
- Disadv. : no possibility to recover the payload after the mission;
- Disadv. : higher costs and risks.

Satellite and Space Station experiment **are analogous but** on ISS:

- ⋄ Bigger detector mass&dimensions ☺;
- ⋄ Fewer launchers and docking possibilities ☹;
- ⋄ Higher geomagnetic cut-off (almost equatorial orbit) ☹!

PAMELA (2006–2016)

Mission Overview

PAMELA (Payload for Antimatter Matter Exploration and Light-nuclei Astrophysics) was the first long-duration space experiment dedicated to high-precision measurements of cosmic-ray antiparticles, nuclei, electrons and positrons.
Launched on a Russian *Resurs-DK1* satellite in June 2006 and operated for almost 10 years in orbit.

Detector Layout

- Time-of-Flight system
- Anticoincidence detectors
- Magnetic spectrometer
- Electromagnetic calorimeter
- Shower tail catcher (S4)
- Neutron detector

Key Capabilities

- Charge sign determination
- Momentum measurement
- Electron/proton separation
- Antimatter searches
- Cosmic-ray composition studies

The PAMELA experiment (2006-2016)

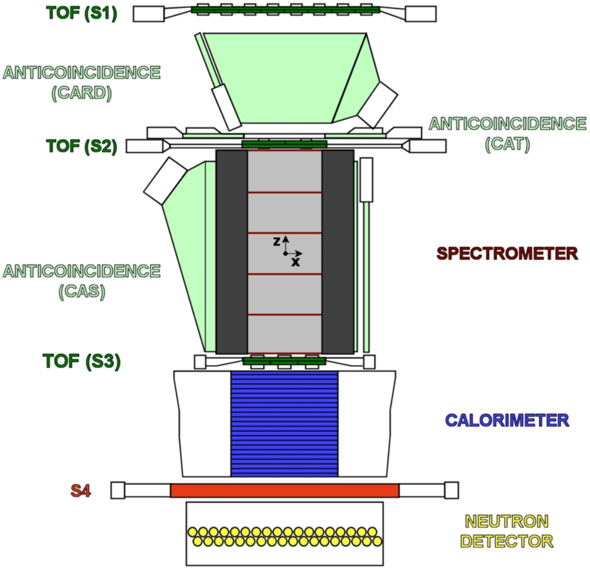

AMS-02: The Alpha Magnetic Spectrometer

Mission Overview

AMS-02 is the largest particle physics detector ever operated in space. Installed on the **International Space Station (ISS)** in May 2011, it performs precision measurements of cosmic-ray particles from sub-GeV to multi-TeV energies.

Detector Concept

- Time-of-Flight
- Anticoincidence system
- Magnetic spectrometer
- Silicon tracker
- Transition Radiation Detector
- Ring Imaging Cherenkov
- Electromagnetic calorimeter

Key Measurements

- Charge sign and rigidity
- Particle velocity
- Electron/proton separation
- Elemental composition
- Antiprotons and positrons
- Search for antihelium and dark matter signatures

The AMS-02 Experiment

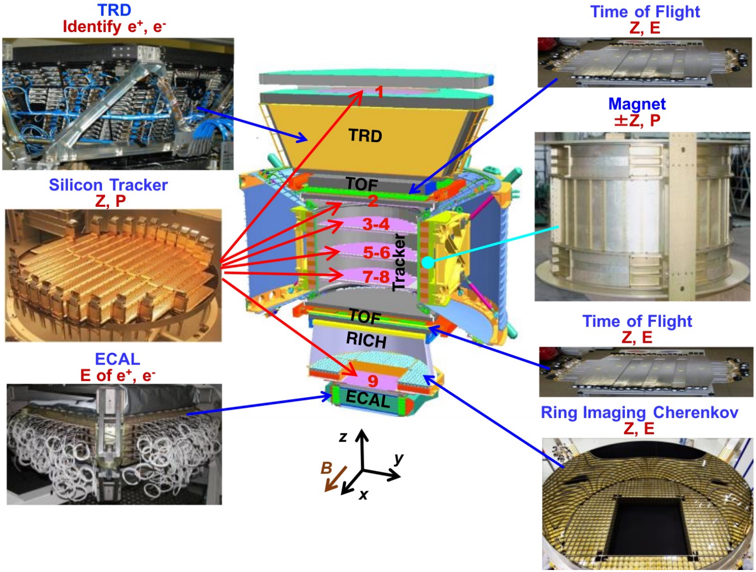

Calorimetric experiments

PAMELA and AMS-02 are experiment based around a **spectrometer**, thus allowing to detect **matter versus antimatter**.

As we have seen already - in parallel to this - scientists use experiments based only on the **calorimetric technique** for the direct determination of charged cosmic rays. This technique allows to **reach higher energies**.

Among many of such experiment, we need to mention **CALET (ISS), DAMPE (satellite), FERMI (satellite) and HEPD-01 and HEPD-02 (satellite)**, still in data-taking like AMS.

Great contributions to Cosmic Ray measurements in recent years have been done also by **ISS-CREAM (ISS) and NUCLEON (satellite)** space missions.

CALorimetric Electron Telescope "CALET"

Launched August 19th, 2015, on ISS. Sensitive to:

- ⋄ electrons: from 1 GeV to 20 TeV
- ⋄ protons and nuclei (up to Z=40): tens of GeV to hundreds of TeV
- ⋄ diffuse gamma emission and GRBs

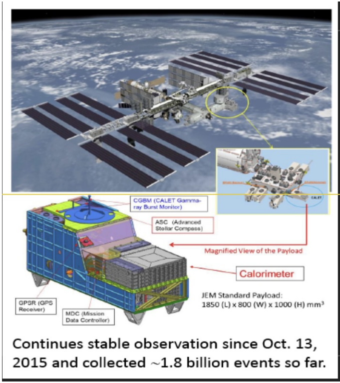

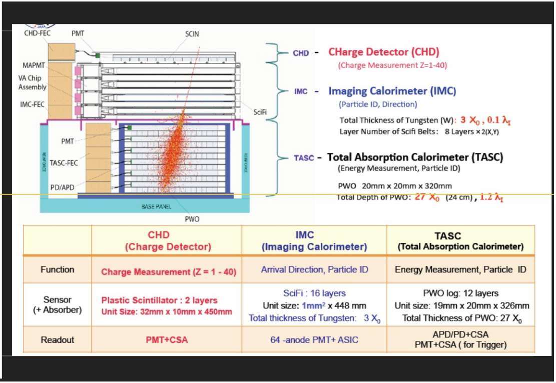

	CHD (Charge Detector)	IMC (Imaging Calorimeter)	TASC (Total Absorption Calorimeter)
Function	Charge Measurement (Z = 1 - 40)	Arrival Direction, Particle ID	Energy Measurement, Particle ID
Sensor (+ Absorber)	Plastic Scintillator : 2 layers Unit Size: 32mm x 10mm x 450mm	SciFi : 16 layers Unit size: 1mm² x 448 mm Total thickness of Tungsten: 3 X_0	PWO log: 12 layers Unit size: 19mm x 20mm x 326mm Total Thickness of PWO: 27 X_0
Readout	PMT+CSA	64 -anode PMT+ ASIC	APD/PD+CSA PMT+CSA (for Trigger)

Launched December 17th, 2015. Sensitive to:

◇ protons and nuclei: 100 GeV – 100 TeV
◇ electrons and gammas: 5 GeV – 10 TeV

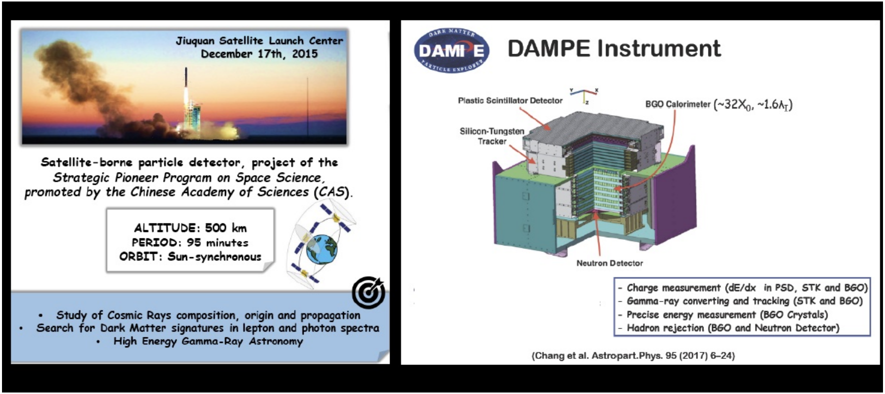

Large Area Telescope LAT onboard "Fermi"

Launched June 11th, 2008.

Gamma-ray space detector, but sensitive to:

◇ electrons and positrons: 20 – 200 GeV

The Fermi Gamma-ray Space Telescope circles Earth every 96 minutes in a 26° inclination orbit at an altitude of 535 km.

Fermi carries two scientific instruments, the Large Area Telescope (LAT) and the Gamma-ray Burst Monitor (GBM).

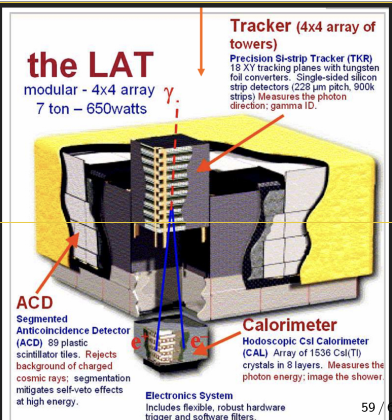

The HEPD on CSES-01 and CSES-02

Launched on Feb. 18th, 2018 and June 15th 2025. Sensitive to

- ◇ protons: 30 - 300 MeV
- ◇ electrons: 3 - 100 MeV
- ◇ light nuclei: up to a few hundreds of MeV

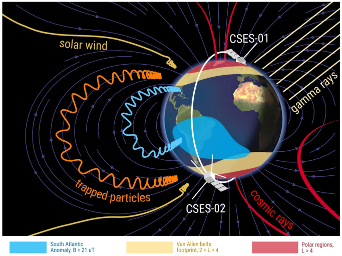

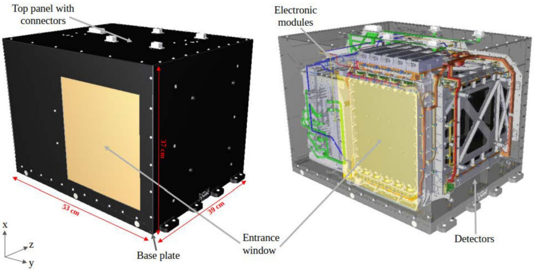

See talk by N. Puccetti for more details

ISS-CREAM experiment (2017 - 2019)

Launched on Aug. 14th, 2017. Sensitive to:

⋄ nuclei ($Z = 1$–26): 1 TeV — 1 PeV.

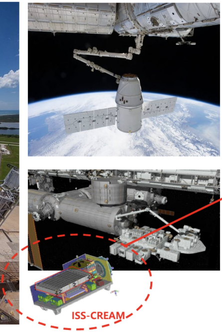

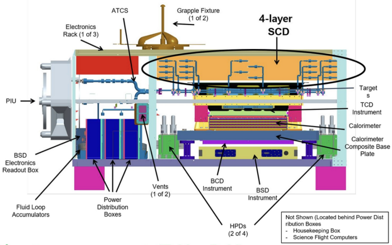

- **Launch : Aug. 14, 2017**
- **Data taken period : Aug. 22, 2017 ~ Feb. 12, 2019 (~ 539 days)**
- **Design to direct measurement of high-energy cosmic rays**

Direct measurement (TeV – PeV)

Silicon Charge Detector (SCD) : Charge measurement, tracking
C-Target & Calorimeter (CAL) : Energy measurement, tracking, trigger
Top/Bottom Counting Detector (TCD & BCD) : e/p separation, trigger
Boronated Scintillator Detector (BSD) : e/p separation by neutron detection

NUCLEON experiment (2014-2017)

Launched on Feb. 18th, 2018. Sensitive to:

◇ nuclei ($Z = 1$–26): 100 GeV — 1 PeV.

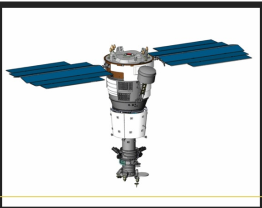

Apparatus mounted aboard the RESURS-P2 satellite.

Sun-synchronous orbit with an inclination of 97° and an altitude of 475 km.

KLEM technique.

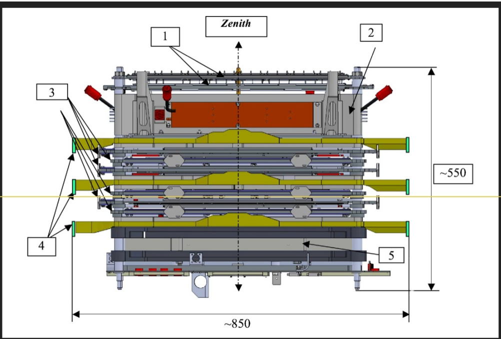

A simplified layout diagram of the NUCLEON spectrometer. 1 – two pairs of planes of the charge measurement system (ChMS); 2 – a carbon target; 3 – six planes of the energy measurement system using the KLEM method (KLEM system tracker); 4 – three double-layer planes of the scintillator trigger system (the trigger system); 5 – a small aperture calorimeter (IC).

Timeline of the major GCRs experiments

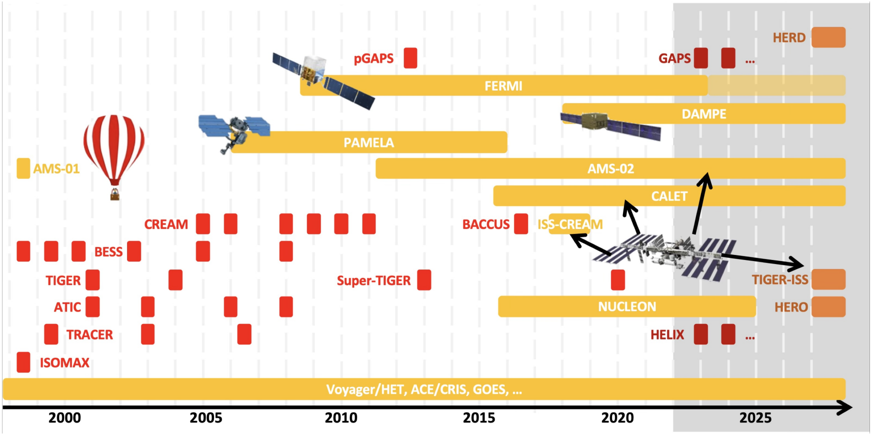

Outline of Lecture 2

In the second lecture, we will talk about:

- Energy Spectrum of CR Protons and Helium
- Heavier nuclei spectra
- Elements with $Z < 40$ and $40 < Z < 56$
- Antimatter measurements in GCRs
- Cosmic Rays in the heliosphere
- Future experiments
- Conclusions